J Wood Sci (2005) 51:209–217
DOI 10.1007/s10086-004-0652-0

ORIGINAL ARTICLE

Yoko Midorikawa · Minoru Fujita

Transverse shape analysis of xylem ground tissues by Fourier transform image analysis II: cell wall directions and reconstruction of cell shapes

Received: November 26, 2003 / Accepted: May 26, 2004

Abstract Cell wall directions of tracheids in transverse sections of *Agathis* sp. and *Cryptomeria japonica* and fiber bodies in *Magnolia obovata* were quantified by Fourier transform image analysis (FTIA). Three kinds of information about cell shapes were determined from the angular distribution functions of the net map-power spectrum pattern (NM-PSP): (1) the peak angle expresses the most frequent cell wall direction, (2) the area of the peak is indicative of cell wall length, and (3) the dispersion of the peak indicates the fluctuation of cell wall orientation. Fluctuations were expressed as the standard deviation (σ) by the use of statistical analysis. Cell wall directions in *Agathis*, that is, directions of the tangential and radial walls (three orientations were detected) were 0° (σ = 7°), 59° (12°), 91° (9°), and 122° (12°), respectively. Pentagonal and hexagonal models were reconstructed as cell shape models in a calculated ratio of 60:40. On the other hand, directions were 0° (5°), 76° (12°), 89° (5°), and 102° (12°) in a calculated ratio of 45:55 in *Cryptomeria*. Fiber bodies were extracted in *Magnolia* and their wall directions were 0° (5°), 50° (7°), 90° (6°), and 131° (7°), respectively. The ordinary accumulated image analysis (OAIA) was checked at the same time in *Agathis*, and indicated that FTIA could be used as a method of reconstruction of cell shape.

Key words Tracheid shape · Fiber shape · Fourier transform · Cell wall directions · Cell shapes

Introduction

The most important structure of wood cells in softwood is the tracheid and the fiber in hardwood as ground tissues, although there are various wood cells. Each represents an important characteristic of the wood. Until now the shapes of these cells, however, were not measured precisely. Fujita et al.[1] developed the Fourier transform image analysis (FTIA) procedure, consisting of a pre-fast Fourier transform (FFT), which clarifies the shape factor by the dot – map and net – map methods, the autocorrelation function from the power spectrum pattern (PSP),[2] and the process of post-FFT, such as polar coordinate analysis. Then they[3] detected the cell arrangement and measured the direction of cell walls (cell sides) according to the process, and tried to reconstruct the most frequent (abundant) cell shape from the PSP maximum power.[2] The accuracy and verification of analysis are unknown. The controlling process of ordinary accumulation image analysis (OAIA) was examined[4] to prevent various errors and quantitative analysis in FTIA was introduced for highly precise quantitative evaluation.[5] We precisely examined cell arrangements of *Agathis* sp., *Cryptomeria japonica*, and *Magnolia obovata*, and determined the grade of fluctuation of it under this process.[6] Dot models and block models were restructured as part of the process. In this report, the most frequent angle of the cell walls (cell sides) was acquired and reconstruction of the cell shapes in transverse sections was performed using the same sample images. The grade of fluctuation was also examined and both data from FTIA and OAIA in *Agathis* were compared in detail.

A number of terms are not defined in this report because of their definition in previous reports.[4–6] Terms specifically defined in this article are shown in Table 1.

Materials and methods

Specimens and picture sampling

Agathis, *Cryptomeria*, and *Magnolia* were analyzed according to our previous report.[6] The same sections and input methods[6] were used in the present study except that microscopic magnification was higher (10×). Pictures of *Agathis*

Y. Midorikawa · M. Fujita (✉)
Division of Forest and Biomaterials Science, Graduate School of Agriculture, Kyoto University, Kitashirakawa-Oiwake-cho, Sakyo-ku, Kyoto 606-8502, Japan
Tel. +81-75-753-6238; Fax +81-75-753-6302
e-mail: kzfujita@kais.kyoto-u.ac.jp

Table 1. Abbreviations and definitions of terms

Abbreviation	Definition
E_{ol}	Overlapping error
ER_{ol}	Error ratio by overlapping
$P_{k=lBW}(\phi)$	Angular distribution function along the low-frequency band width ($17 \leqq k \leqq 64$)
$P_{k=mBW}(\phi)$	Angular distribution function along the middle-frequency band width ($65 \leqq k \leqq 256$)
$P_{k=hBW}(\phi)$	Angular distribution function along the high-frequency band width ($257 \leqq k \leqq 512$)
$P_{ac}(\phi)$	Angular distribution function after angle compensation
r_1, r_f, r_2	Type of radial walls on cell shape models. Radial wall 1 and floor-type radial wall and radial wall 2, respectively
A_{peak}	Peak area. Ar_1, Ar_f and Ar_2 are peak areas of r_1, r_f, r_2, respectively
Lr_1, Lr_f, Lr_2	Lengths of r_1, r_f, r_2 walls

and *Cryptomeria* were directly input to Luzex III (Nireco) through a monochrome television camera (Ikegami ITC530), to give a one-pixel width on the CRT screen of 1.39 μm, with an input area of 1.42 × 1.42 mm. There were about 35 tracheids along the radial direction, and mainly contained an earlywood zone and a small area of the latewood zone in *Agathis*. Latewood-like zones were observed repeatedly, although *Agathis* is one of the tropical trees. One thousand tracheids were sampled at a time. There were about 20–25 tracheids along the radial direction and the total number of cells was about 700 in *Cryptomeria*. They consisted of almost all earlywood cells. *Magnolia* was input to Luzex III through a film scanner Polascan 4000 (Poraroid, 1280 dpi) and image processing software, Photoshop.v.5.0J with a pixel width of 0.83 μm (sample area 0.85 × 0.85 mm). On the other hand, for the OAIA examination of *Agathis* sections, only the earlywood area was selected and input under the same conditions as *Magnolia*.

Extractions of the structure element and shape factor, and their PSP analysis

A transverse image of *Agathis* was transferred to a binary image as a wall map (WM)[4] (Fig. 1a), and simplified to a net map (NM)[4] (Fig. 1b) after removal of rays according to previous reports.[2–4] The same treatments were performed for *Cryptomeria*. Furthermore, the NM was divided into fragment maps (FM)[4] of tangential walls (Fig. 2a) and of radial walls (Fig. 2c) by cutting off at the corner map (CM)[4] in order to measure the length and direction of cell sides by OAIA. A selective net map (sNM) (Fig. 1e) was created for *Magnolia* (Fig. 1d) as previously described[6] for extraction of only the body part of the wood fibers.

These maps were transformed to the PSPs by FFT processing (Fig. 1c,f). These PSPs were used for the polar coordinate analysis as programmed by Maekawa et al.[2,3] and angular distribution functions were obtained (Figs. 3, 4, 5a).

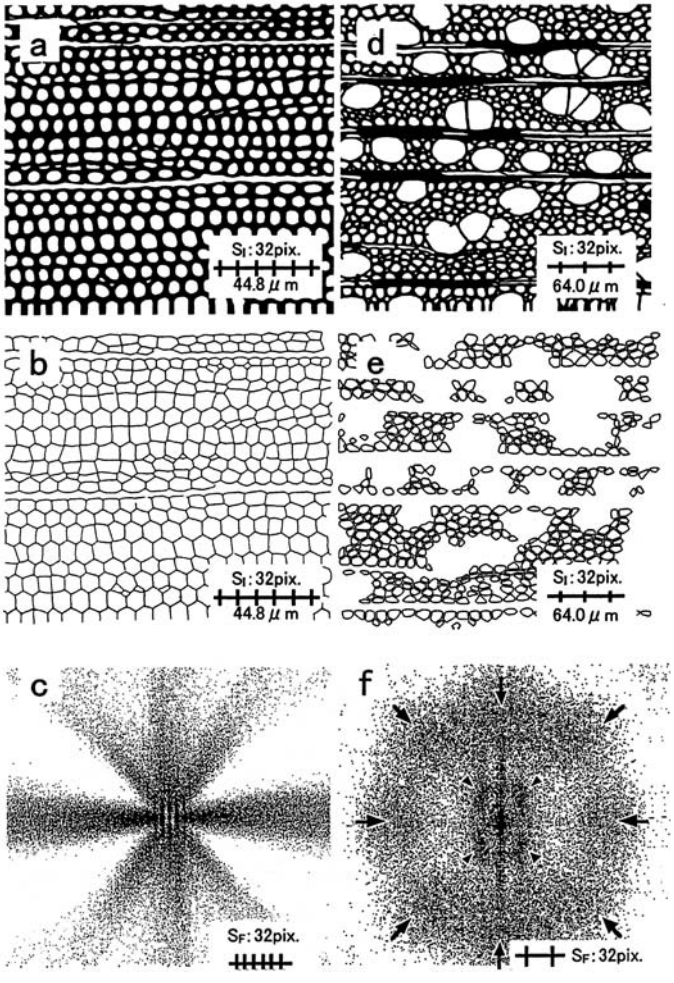

Fig. 1a–f. General procedure of Fourier transform image analysis (FTIA) for direction analysis. **a** Wall map (WM), **b** net map (NM), **c** power spectrum pattern (PSP) of **b** in case of *Agathis* sp. **d** WM, **e** selective NM (sNM), called a body-NM, and **f** PSP of **e** in case of *Magnolia obovata*. Note that NM-PSP (**c**) provides spreading power from the origin to the high-frequency bandwidth in a star-like fashion in eight directions in *Agathis*. On the other hand, sNM-PSP (**f**) shows that the power is distributed in a circular fashion and some spots are discerned on the circle (*arrowheads*) and further spots exist on the higher frequency power ring (*arrows*) in *Magnolia*

Results and discussion

Overall information of NM-PSP

Structure elements on a NM are cell sides and they contain three types of shape factors, that is, length, direction, and arrangement. When NM-PSP of *Agathis* and *Cryptomeria* are surveyed in the low-frequency band width (IBW, $17 \leqq k \leqq 64$), there are signs similar to DM-PSP on which arrangement information appears. We can see star-like rays spreading in eight directions from the origin to the middle-frequency and high-frequency band widths (mBW: $65 \leqq k$

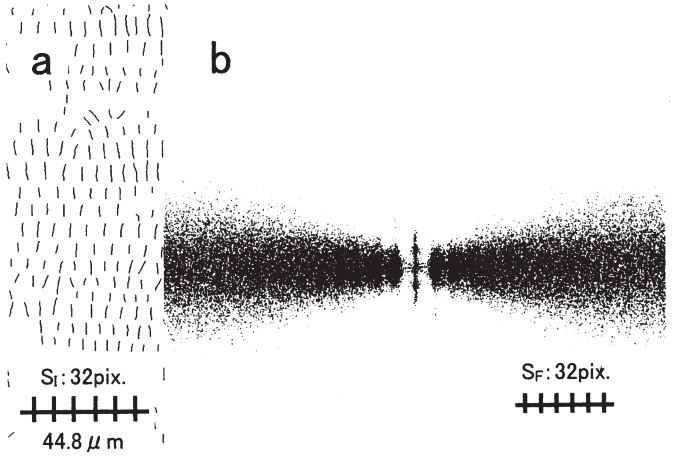

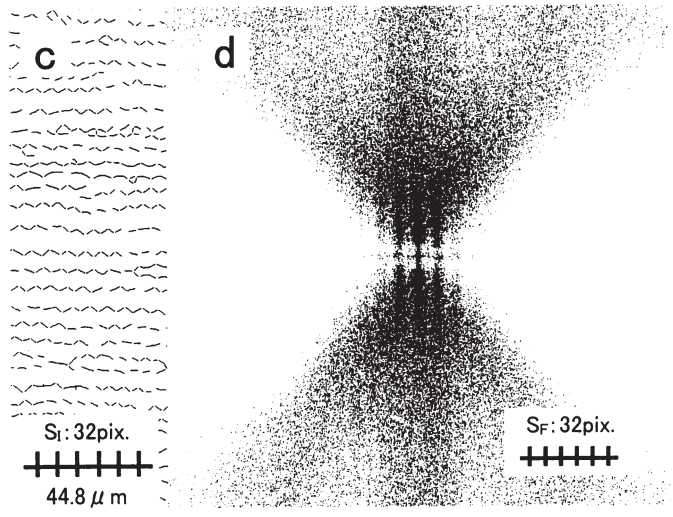

Fig. 2a–d. Fragment maps and PSPs of *Agathis* sp. **a** Fragment map of tangential walls (t-FM), **b** PSP from **a**, **c** fragment map of radial walls (r-FM), and **d** PSP from **c**. Note that power concentrates on the equatorial direction in **b**. On the other hand, power fans out from the meridian direction in **d**. The direction of power crosses the direction of cell sides perpendicularly

≦ 256, hBW:257 ≦ k ≦ 512). These power radiations inform us of the length (l) and direction (θ) of the wall sides (Fig. 1c). On the other hand, eight spots are observed along a ring in the mBW on the PSP of *Magnolia* sNM (Fig. 1f). The ring corresponds to the paired lines of five-pixel width and spots on the ring originate from the wall direction (θ).

Concentration and diffusion of the power were calculated more quantitatively, that is, $P_{k=\mathrm{hBW}}(\phi)$ in *Agathis* and *Cryptomeria*, and $P_{k=\mathrm{mBW-hBW}}(\phi)$ in *Magnolia* (Figs. 3, 4, 5a), in order to examine only cell side lengths and directions without arrangements.

Here, we note that three kinds of keys relating to cell shape are expressed on the peaks of $P(\phi)$. Namely, key 1 is $\phi_{\max}$. It shows the most frequent direction ($\theta_{\max}$) of the cell wall, i.e., $\theta_{\max} = \phi_{\max} \pm 90°$. Key 2 is the peak area. It has a proportional relation to the integrated length of each cell wall, although the proportionality coefficient is not known. Because a cell side that has a one-pixel width is treated as a

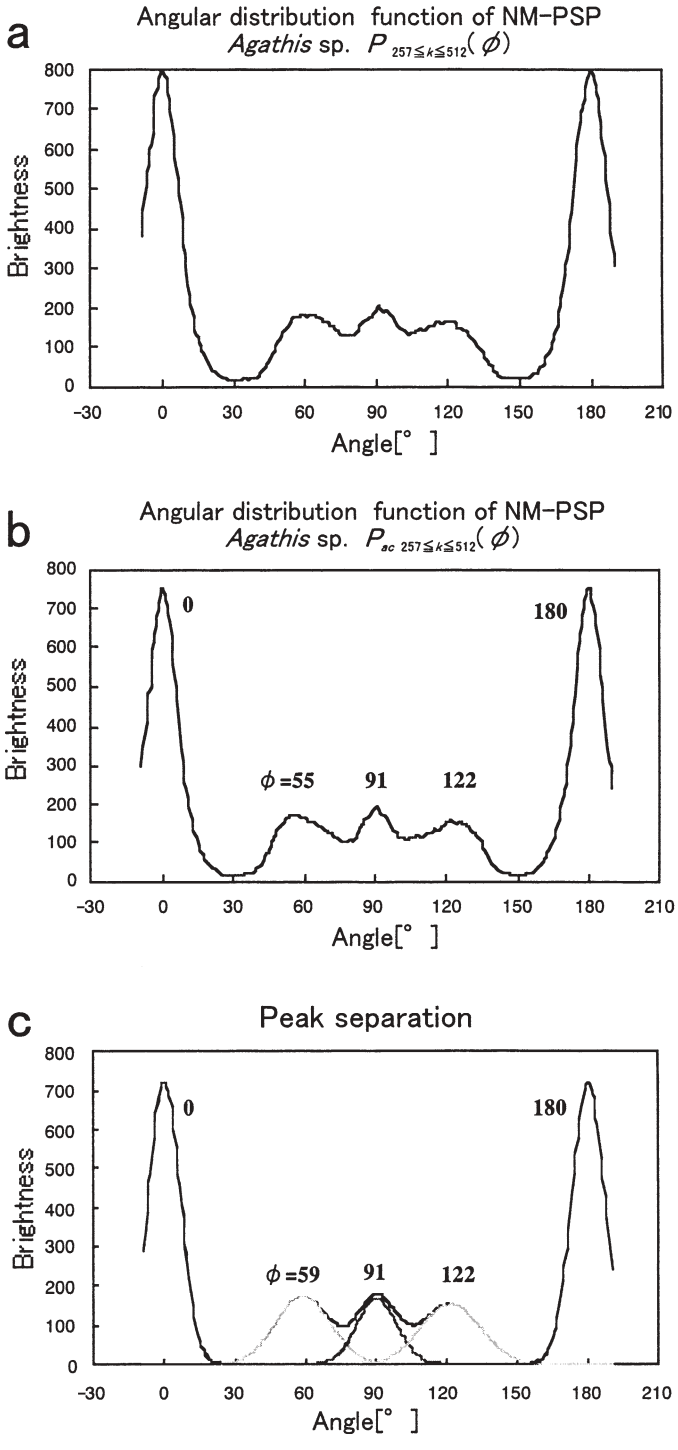

Fig. 3a–c. The NM-PSP analysis of *Agathis* sp. **a** Raw angular distribution function, **b** angular distribution function after angle compensation, and **c** angular distribution after peak separation composed of five Gaussian peaks. Compensation was done by using the test patterns similar to the structure element of NM (**b**). It was used in fluctuation analysis because **c** consisted of normal distribution curves. R (correlation coefficient) = 0.997

σ function and there is no power decrease, that is, no missing order, the relation is kept in whole bandwidth. Key 3 is the peak dispersion expressing the fluctuation of wall directions from $\theta_{\max}$.

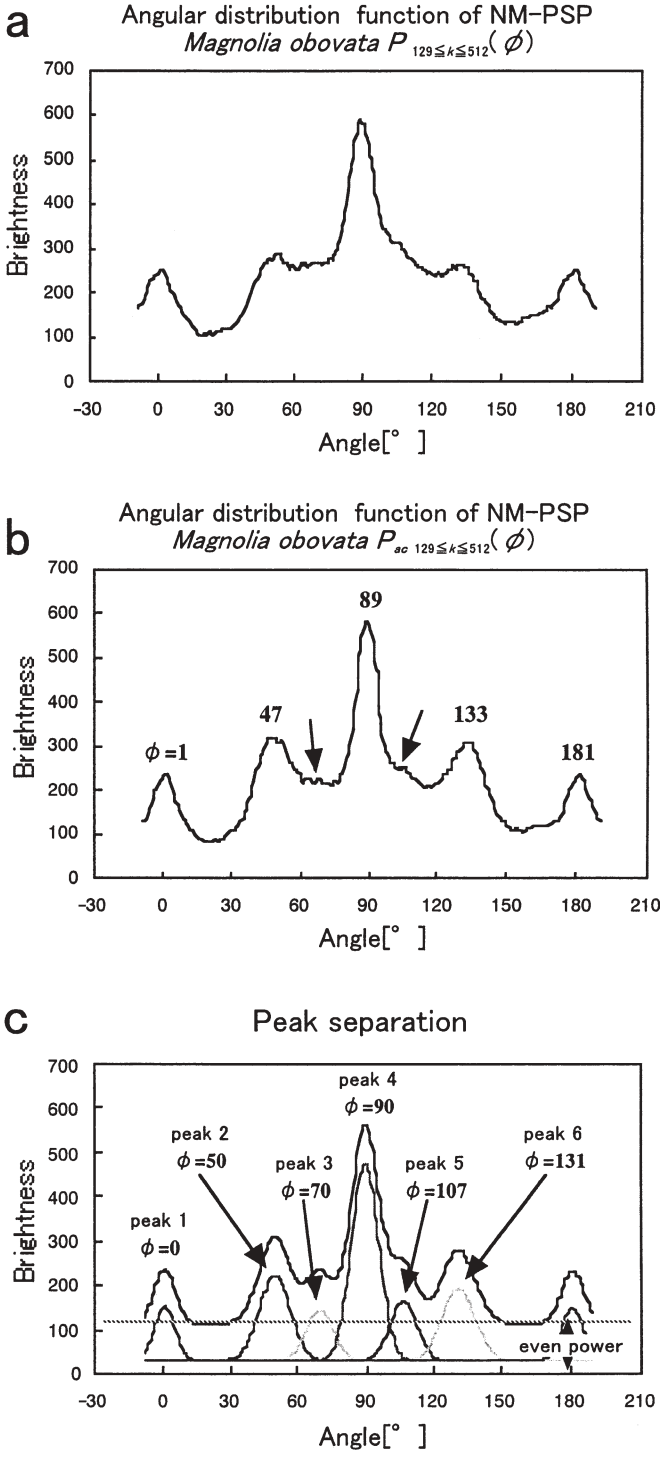

Fig. 4a–c. The NM-PSP analysis of *Magnolia obovata*. **a** Raw angular distribution function, **b** angular distribution function after angle compensation, and **c** peak separation composed of five Gaussian peaks. Compensation was done by using the test patterns similar to the structure element of NM (**b**). Even power indicates that there are many cell sides not identified in **c**. $R = 0.978$

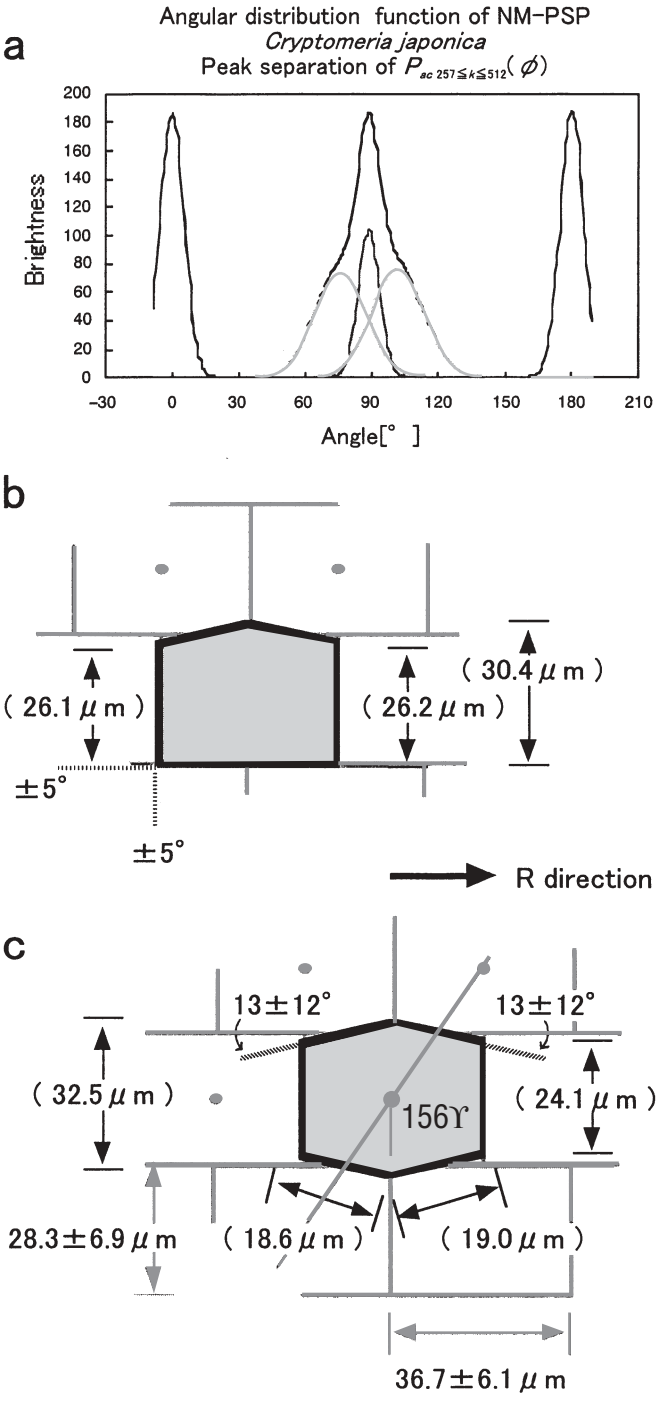

Fig. 5a–c. The NM-PSP analysis and reconstruction of *Cryptomeria japonica* tracheid cross shape. **a** Angular distribution after peak separation composed of five Gaussian peaks, **b** pentagonal (house) model, and **c** hexagonal model. Cell side directions and standard deviations σ are added. Values in parentheses are calculated data from models. House model: hexagonal model = 45.2: 54.8

Experimental conditions for transverse shape analysis

The FTIA enables us to pull out certain features from ambiguous structures when many samples are prepared. We tried to input as many tracheids as possible in order to enhance the reliability of the angular distribution function.

For this purpose, lower magnification of picture sampling is desirable within the optical resolution R_O and discrete resolution R_D.[4] A wider sampling area sometimes contains undesirable heterogeneous parts. Therefore, in this report, we decided not to make the observations under such low magnification and repeated the samplings mainly from the homogeneous earlywood zone. As the PSP from each NM is very weak, low power is omitted by digitally processing of the gray levels. This problem was overcome[5] by overlapping different NMs from several areas, although some convolution techniques were introduced.[6] The overlapped NM image will generally become very complicated. This procedure, however, is expected not to bring serious influences, being based on the Fourier transform theory, in which phase information of the spatial domain is eliminated in the power spectrum. Fujita et al.[7] verified this characteristic by the method of optical Fourier transform, and reported that overlapped sections also generated the original periodicity in diffraction. This characteristic was also applied to electron diffraction of cellulose crystals.[8] Midorikawa and Fujita[9] cut off maps of only the earlywood zone of softwood into long and slender strips along the tangential direction and overlapped them. Then they demonstrated that they could increase the number of tracheids, holding the uniformity of a sample. The negative influence of overlapping (E_{ol}, overlapping error) must be estimated beforehand.

This error must originate from the overlapped points between cell sides on two NM sheets (NM_1 and NM_2), because these points having two times the contrast are again transferred to binary data. When the ratio of lines are m_1 and m_2 on NM_1 and NM_2, the probability of overlapping is $m_1 \times m_2$, namely m^2 in the homogeneous NMs. The line position is only a few percent in the area on each NM. The overlapping probability of over two sheets, that is, m^{over2} becomes negligible when this theory is expanded to numerous sheets (NM_n) and the line ratio m is under 0.1. The error ratio of overlapping ($ER_{ol(1+2+3+\ldots+n)} = ER_{oln}$) is determined by the following formula.

$$ER_{oln} = (n-1)m/2 \tag{1}$$

The curves of ER_{ol} in the case of $m = 0.01$, 0.05, and 0.1 are shown in Fig. 6. In this report, m was about 0.05. The error ratio does not exceed 0.1 even if five sampling images are overlapped.

The most severe problem in cell shape analysis is the angular error that is caused by oblique lines.[5] Power is underestimated by around 50% at oblique directions, which is unavoidable in the present FFT systems. The degree of underestimation of powers was detected by using test patterns similar to cell side fragments that are the structure element of NM in order to minimize the negative influence. This modified angular distribution function that performed angle compensation was written as $P_{ac}(\phi)$. One thousand line segments with 1-pixel width and 30-pixel length were spread randomly on a screen as the test (Fig. 7a). These segments can be treated as a σ function.[4,5] From the PSP of this map (Fig. 7b), angular distribution functions were obtained from the same frequency bandwidth as that of the real NM-PSP. This operation was repeated 50 times (a total of 50 000 lines). We compensated the original angular distribution function $P(\phi)$ to the modified function $P_{ac}(\phi)$ using the curve (Fig. 7c). Because the PSP outputted power with point symmetry, the $0 \leqq \phi \leqq 180°$ display was sufficient

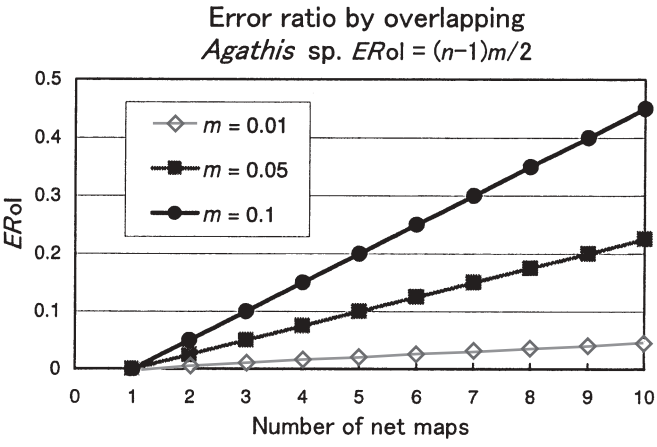

Fig. 6. Examination of error ratio caused by overlapping (ER_{ol}). In the case of *Agathis* sp. that has an area ratio of about 0.05, five maps can be overlapped at less than 0.1 error ratio

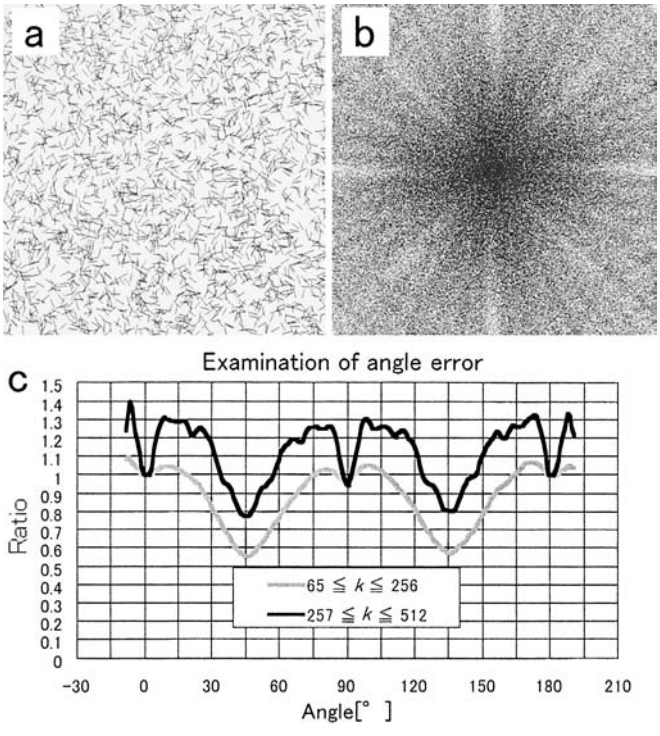

Fig. 7a–c. Examination of angle error by using fragment test patterns. **a** Many fragments of constant length are dispersed randomly, **b** PSP of **a**, and **c** angular distribution functions of **b** along the middle-frequency and high-frequency bandwidths. The y-axis expresses the ratio of power level considering the level at 0° as 1 in **c**. Curves on the high-frequency bandwidth were used to compensate for the raw angle distribution functions because the raw functions were traced along the same bandwidth

for $P_{ac}(\phi)$. Peaks were detected at around 0° and 180° in both species, and Figs. 4, and 5 show the range of $-30° \leqq \phi \leqq 210°$.

Direction analysis of cell wall and reconstruction of transverse cell shape

Reconstruction of tracheid shape in *Agathis* was performed from ϕ_{max} values of $P_{ac}(\phi)$ using key 1. The wave separation software Sigma Plot, v.5.0 was used on the assumption that each peak has a normal distribution curve in this analysis. Maximum directions of peak (ϕ_{max}) after the separation were slightly different from those before the separation in *Agathis* (Fig. 3). They were adopted for the model reconstruction. The tracheid arrangement models (block models) that were previously proposed[6] were used as the base of reconstruction here and we added the information of cell wall directions (θ) to them by the ϕ_{max}. The FM and FM-PSP of *Agathis* are shown in Fig. 2 and demonstrate the relation between cell wall direction (θ) and power direction (θ). When FM is compared with FM-PSP, power is concentrated on the direction (ϕ) (Fig. 2b,d) perpendicular to the direction of cell sides (θ) (Fig. 2a,c). It is clear that NM-PSP (Fig. 1c) consists of t-FM-PSP (Fig. 2b) and also r-FM-PSP (Fig. 2d). Here, it must be remembered that the radial direction was set by the horizontal direction of the screen ($\theta = 0°$) and $\phi = \theta \pm 90°$ in the frequency domain (Fig. 2b,d).

Tangential walls were set around $\theta = 90°$ in the picture sampling. It is clear that sharp peaks at $\phi = 0°$, 180° are generated from tangential walls shown in Fig. 3. On the contrary, as for radial walls, six radiations were observed (Fig. 1c) and three peaks at 59°, 91°, and 122°, and their point symmetric peaks could also be identified (Fig. 3c). Direct interpretation of this NN-PSP is an octagonal cell shape. Such cells are rare on the actual transverse section, so we can conclude pentagonal cells in the shape of a house composed of two walls (tangential walls), one flat floor (r_f) corresponding to $\phi = 91°$ (Fig. 3c), and two oblique roofs of $\phi = 59°$ (r_2) and 122° (r_1) (Fig. 8a). The same method was used in the case of *Cryptomeria*. The data are shown in Table 2.

The floor is not of a strict geometry but contains various cases. At the tracheid tips, radial walls are often flat and their tangential walls are very short. Transverse cell shapes are a slender rectangle. We omit such cases in the discussion because of their rare occurrence. Tracheids neighboring rays have a straight radial wall, and result in the house-like shape. When radial files are in contact with each other, many tracheids have a typical roof shape, composed of two sides. The two sides, however, were often uneven in length and the longer ones became flat (Fig. 8b). Moreover, the included angles between the two radial walls are often very large, near 180°, even if they have similar length. When the main peak at around 90° in *Cryptomeria* was separated into two peaks, the distance between them was only 4° (Fig. 5a). Although such evaluations will be reported in a following report, the large peak was calculated as one floor having some angular fluctuations in this report. We therefore categorized them to the house model. The house model was reconstructed by the rotation of r_1 and r_2 of the block model around the middle point of each roof side and stopped in the position at 59° and 122°. Each side is elongated to the crossing points of rotated sides. The hexagonal cell shapes are also abundant in the original picture judging from the peak area ratio between r_1 and r_2 and r_f, resulting in the figure consisting of every two-faced cell wall as a whole.

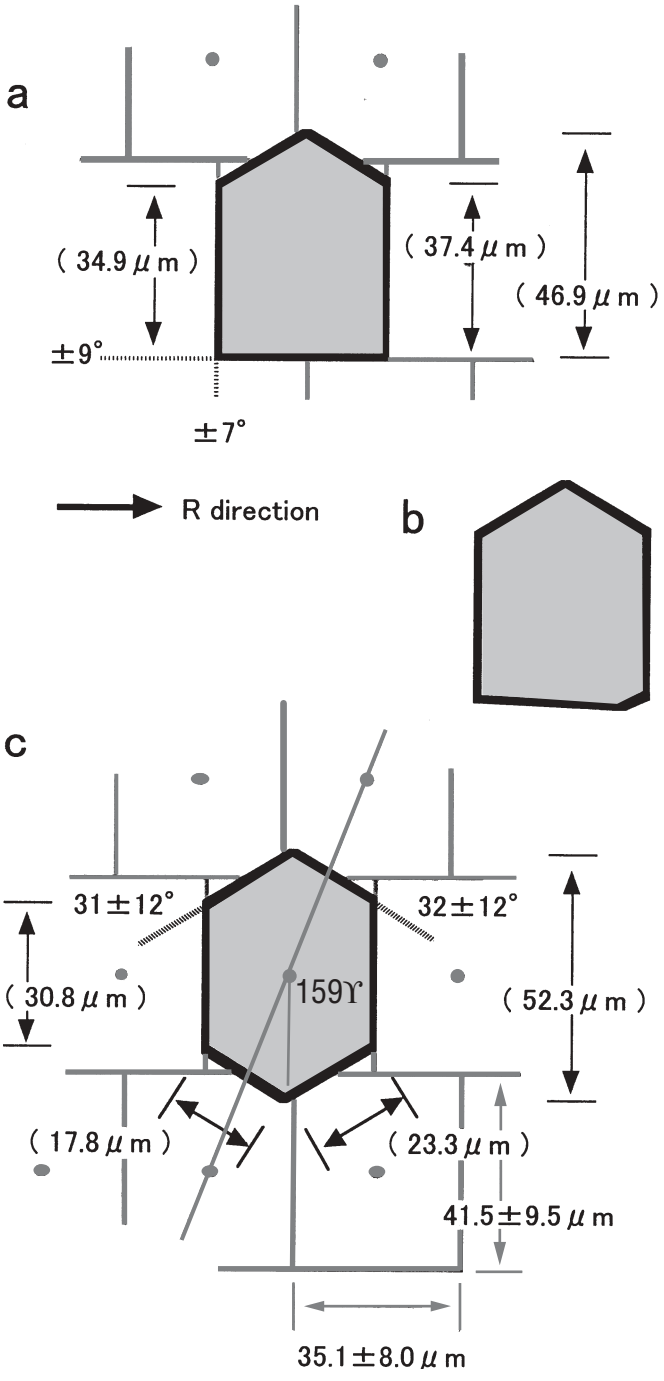

Fig. 8a–c. Reconstruction of *Agathis* sp. tracheid cross shape. **a**, **b** Pentagonal (house) model, and **c** hexagonal model. Cell side directions and standard deviations σ are added. Values in parentheses are calculated from models; **b** is categorized as a house model although the floor contains two sides. House model: hexagonal model = 40.1: 59.9

Table 2. Angles of cell walls calculated from the angular distribution function of net map-power spectrum patterns (NM-PSPs)

	Peak angle (ϕ) and σ of NM-PSP's angular distribution function (°)						Slope of radial walls		
Agathis sp.	0 ± 7	59 ± 12		91 ± 9		122 ± 12	32	0	31
Peak name	t	r_2		r_f		r_1	r_2	r_f	r_1
Area ratio	3.1	1.4		1		1.3			
Cryptomeria japonica	0 ± 5	76 ± 12		89 ± 5		102 ± 12	13	0	13
Area ratio	1.9	1.7		1		1.8			
Magnolia obovata	0 ± 5	50 ± 7	70 ± 6	90 ± 6	107 ± 6	131 ± 7	40	0	41
Peak name	Peak 1	Peak 2	Peak 3	Peak 4	Peak 5	Peak 6	Peak 2	r_f	Peak 6
Area ratio	0.1	0.5	0.3	1	0.3	0.4			

Each power was generated from tangential wall (t) and radial walls (r_2, r_f, and r_1)

$P_{ac}(\phi)$ of *Magnolia* (Fig. 4) was quite different from that of *Agathis* (Fig. 3) and *Cryptomeria* (Fig. 5a) when it was observed. Four peaks are very sharp in the range $0° \leqq \phi < 180°$, and small shoulders are also discernable around 75° and 105° (arrows in Fig. 4b). Then, it was separated into six peaks (peaks 1–6 in Fig. 4c and Table 2) using Sigma Plot, suggesting a dominant octagonal cell shape. Cell arrangement and shape are more complicated in hardwoods than in softwoods for three main reasons: (1) transverse expansion of the vessels, (2) elongation of wood fiber tips, and (3) ray distribution. Vessels are very abundant; more than 100/mm^2 in *Magnolia*. The cell arrangement and shape are also affected by tip invasion into the cell corner from upper and lower fibers. The neighboring radial walls with rays are flat. Small invading tips were often observed at the corner position between ray and two fibers, and these may have derived the small peaks 3 and 5. In particular, peak 4 had small angular fluctuations in the radial walls that were flattened by the neighboring rays. When Fig. 4b,c is observed, powers dispersed in all directions are equal to the amount of peaks 1–6, suggesting that many cell sides are not yet identified. For the reasons described above, it is difficult to reconstruct the correct cell shape of fiber bodies and so only data is given in this report.

Existence ratio of transverse cell shape models

The peak areas (A_{peak}) correspond to the accumulation length of each cell wall as stated above. Then, we examined the existence ratio of transverse cell shape models from peak areas in *Agathis*. We focused on the r wall only, and computed the following process in order to simplify calculations. The area of each peak r_1, r_f, r_2, namely, Ar_1, Ar_f, Ar_2, was calculated from the angular distribution function (Fig. 3c) after their peak separation. When the existence ratio of the house model and hexagonal model were set as x%, y%, and wall length in house model as Lr_1, Lr_f, Lr_2, respectively, the following relations are:

$$x + y = 100 \tag{2}$$

$$(Ar_1 + Ar_2)/Ar_f = (x + 2y)(Lr_1 + Lr_2)/xLr_f \tag{3}$$

In Eq. 3, the left side expresses peak area ratio of oblique walls (r_1, r_2) against the flat wall (r_f) , and the right side shows the wall length ratio. From Eqs. 2 and 3 x and y were 59.9% and 40.1%, respectively (Fig. 8). The fact that the house model is much abundant than hexagonal model is very attractive. Tracheids with a house model shape existed at various places, in addition to both sides of the rays when the NM of a transverse section was observed. On the other hand, the house model was less abundant than the hexagonal model, 45% and 55%, respectively, in *Cryptomeria* (Fig. 5a,b). The existence of the rectangular model was ignored in the above-mentioned operation process, because the influence will be only slight because of its rare existence.

Fluctuation analysis of tracheid shape

Fluctuations in cell arrangement were analyzed previously[6]. Here, the fluctuation in cell wall direction is analyzed. We regarded $B(x, y)$, representing the distribution of DM, as the periodic function.[6] $P(k, \phi)$ was finally translated into the periodic distribution function *Period* (τ, ϕ). Disorders of periodicity were expressed as a standard deviation by considering a normal distribution of the functions. Objects are considered as nonperiodic in the direction analysis of the cell wall. Each cell side causes two power radii perpendicular to the cell side from the origin of the PSP. Thus, it was sufficient to read $P(\phi)$.

We required a position equivalent to the standard deviation σ and evaluated the fluctuation in *Agathis* shown in Fig. 3c and *Cryptomeria* shown in Fig. 5a (Table 2) using a normal distribution analysis.[6] Consequently, radial walls r_2, r_f, and r_1 had fluctuations of 12°, 9°, and 12° for sides from 59°, 91°, and 122°, respectively, while tangential wall t was 7° smaller than the radial walls in *Agathis*. On the other hand, radial walls are 12°, 5°, and 12° from 76°, 89°, and 102°, and the tangential wall was 5°, which was equal to r_f in *Cryptomeria*.

Comparison between cell shape models by FTIA and OAIA

Cell arrangement was previously evaluated quantitatively by FTIA[6] and cell shape is characterized by FTIA in this report. FTIA itself was a new analysis method and there are many preconditions. Then, the provability of reconstruction of cell shape models should be inspected by OAIA, a conventional analysis method, also using the data of Table 2 in

Table 3. Comparison between Fourier transform image analysis (FTIA) and ordinary accumulation image analysis (OAIA) in *Agathis* sp.

Parameters	FTIA			OAIA
	House model	Average	Hexagonal model	
Feret's $H \pm \sigma$ (μm)	–		–	38.9[a] ± 6.5
Feret's V (μm)	–		–	49.0
r-dia compensated from Feret's H (μm)	–		–	36.3[b]
r-dia $\pm \sigma$ in block model (μm)	35.1[a] ± 8.0		35.1[a] ± 8.0	–
Area (μm^2)		1.46×10^3[c]		1.51×10^3[d]
t-dia $\pm \sigma$ in block model (μm)	41.5[a] ± 9.5		41.5[a] ± 9.5	–
t-dia minimum (μm)	(35.7, 36.5)	32.9	(30.8)	25.7[e]
t-dia maximum (μm)	(46.9)	50.1	(52.3)	–
$r_1 \pm \sigma$ (°)	31 ± 12		31 ± 12	35 ± 9[f]
$r_2 \pm \sigma$ (°)	32 ± 12		32 ± 12	38 ± 9[f]
Ratio between two models (%)[g]	40.1		59.9	–

Figures in parentheses are calculated from models
σ, Standard deviation
[a] Median value of Gaussian distribution (the others are most frequent values)
[b] Compensated value from overestimated Feret's H (2.6μm) generated by t-wall inclination (average 84.3°)
[c] Calculated with consideration of ratio between two models
[d] Compensated value by the addition of half value of IM area
[e] Arithmetic mean value
[f] Calculated from length sum
[g] Calculated from area ratio of inclining radial walls against flat radial wall at angular distribution function and wall length ratio of models

our previous report.[6] *Agathis* was analyzed as an example. A very wide region containing about 6600 tracheids was used[6] as sample images in FTIA analysis. About 1000 tracheids were sampled on one screen and then two screens were overlapped in this study. On the other hand, OAIA measurement became possible only after strict separation of each element. These separations are very troublesome. Prudent sampling under higher magnification is necessary for the separation. As already described, especially in OAIA, sampling regions were limited and the number of tracheids was about 350. In the pure earlywood region, the OAIA sample consists of slightly larger tracheids along the radial direction than the tracheids used for the FTIA analysis. When this fact is taken into consideration, it can be regarded that the results of both analyses in Table 3 are consistent. Some items will be examined in more detail.

In comparison of radial diameters, because tracheids are produced constantly from the cambium forming the radial files, the radial diameter measured by OAIA is expected to be identical to the radial periodicity estimated by FTIA; that is, the radial interval of the block model. Feret's diameter H seems to be the most easily measured (Feret's H in Table 3). Tangential walls are sometimes inclined, and their inclinations result in an overestimation of radial diameters. Although direction measurements of short lines are very difficult in OAIA, especially under low magnification, the results for t, r_1, r_f, and r_2 are shown in Table 3. Feret's H data were compensated (r-dia compensated from Feret's H in Table 3). As a result, the OAIA measurement of 36.3μm was 3.4% larger than the FTIA measurement of 35.1μm. The difference must reflect the sample characteristics, because large tracheids were selectively sampled from pure earlywood in OAIA.

In comparison of cell areas, we examined the validity of models from the area information. When transverse sections of the house and hexagonal models were computed considering the existing rates of 59.9% and 40.1%, respectively. Total area average was calculated to be $1.46 \times 10^3 \mu m^2$. On the other hand, in the OAIA measurement, the expanded lumen map (e-LM)[4] separated by intercellular layer map (IM) was used. Data must be compensated for by the addition of a half value of the IM area surrounding each tracheid. Then, it became $1.51 \times 10^3 \mu m^2$ and was 3.4% larger than FTIA models of $1.46 \times 10^3 \mu m^2$ (Table 3). Rays are counted in the t-diameter by the periodicity of FTIA, and are thought to have weak influence because they occupy a large part of the xylem. The 3.4% inconsistency seems to be due to the reason described above.

In comparison of cell side lengths, the result was considerably different between OAIA and FTIA (t-dia minimum in Table 3). The length of the t-fragment measured by OAIA was estimated to be 25.7μm. On the other hand, tangential wall length was calculated to be 32.9μm when the ratio of both models was considered by FTIA. The result of OAIA was smaller by 25%, when both data were compared. Very short t-fragments of tracheid tips must be the main reason for this underestimation. Moreover, fluctuations of r_1 and r_2 in FTIA were 12°. If the angle of r_1 and r_2 is corrected to a slightly steep slope, a tangential wall suddenly becomes short. OAIA angles of r_1 and r_2 were larger by 4°–6° according to FTIA. Feret's V, however, was consistent with the t-dia maximum. Determining the lengths of the cell sides calculated from angles still has some problems. Comparison of the FTIA with OAIA results (Table 3) indicates that the data are similar except for only a few cases, in spite of the complete independence of both analytical processes. Thus, it can be concluded that FTIA is appropriate for the quantitative evaluation of softwood tracheids. A large number of structure elements can be analyzed in a short time by FTIA, so it is suitable for the analysis of the most frequent value and also the fluctuation.

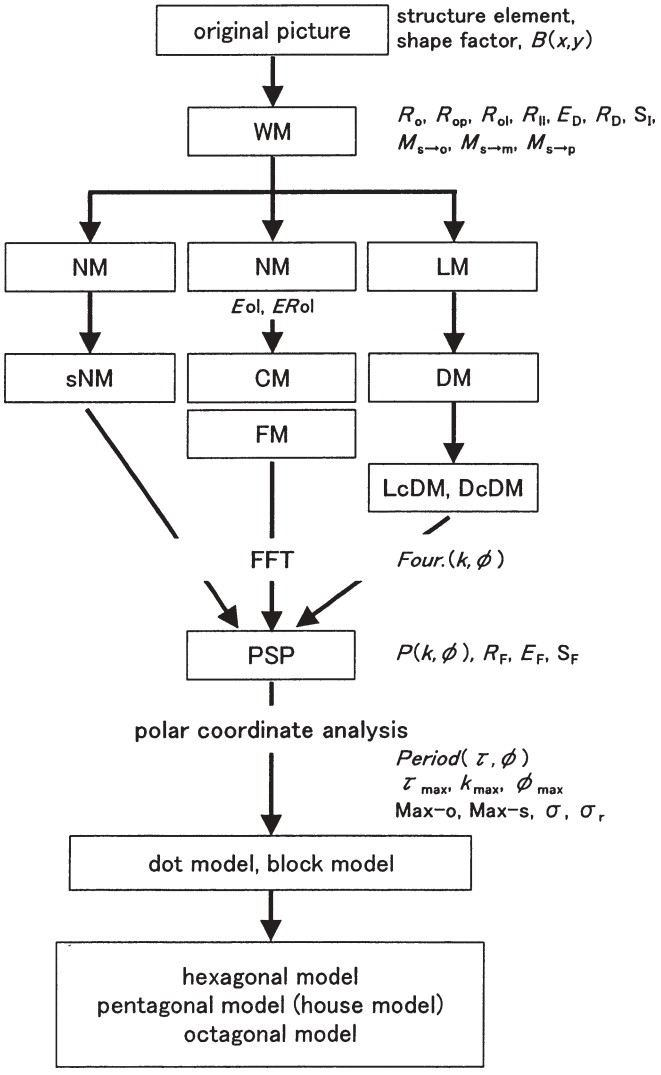

Fig. 9. General series of FTIA for transverse shape analysis. The procedure shows maps, patterns and models (*in rectangles*), and terms and functions from previous reports[4–6] and the present study

Then tracheid cell-shape models of many species from all over the world will be represented by FTIA in a following report. This method can also be applied to other softwoods because softwoods consist of very uniform cells. Analysis is very difficult in hardwoods, however, because rays, vessels, and tips disturb cell arrangements and E_{spn} is inevitably generated. Some problems remain when the method is used for all species, but these problems are expected to be resolved. The FTIA series from this report and our previous work[6] are shown in Fig. 9 as a conclusion.

References

1. Fujita M, Kaneko T, Hata S, Saiki H, Harada H (1986) Periodical analysis of wood structure I: some trials by the optical Fourier transformation (in Japanese). Bull Kyoto Univ Forest 60: 276–284
2. Fujita M, Saiki H, Norimoto M (1991) Anisotropic periodicity analysis on cell distribution and microfibril orientation by the various diffraction methods. Grant-in-Aid for Scientific Research (Category B) Result Report from Japan Society for the Promotion of Science
3. Maekawa T, Fujita M, Saiki H (1993) Characterization of cell arrangement by polar coordinate analysis of power spectral patterns (in Japanese). J Soc Mater Sci Jpn 42:126–131
4. Fujita M, Midorikawa Y, Ishida Y (2002) Experimental conditions for quantitative image analysis of wood cell structure I: evaluation of various errors in ordinary accumulation image analysis (in Japanese). Mokuzai Gakkaishi 48:332–340
5. Midorikawa Y, Fujita M (2003) Experimental conditions for quantitative image analysis of wood cell structure IV: general procedures of Fourier transform image analysis (in Japanese). Mokuzai Gakkaishi 50:73–82
6. Midorikawa Y, Ishida Y, Fujita M (2005) Transverse shape analysis of xylem ground tissues by Fourier transform image analysis I: trial for statistical expression of cell arrangements with fluctuation. J Wood Sci 51:201–208
7. Fujita M, Hata H, Saiki H (1991) Periodical analysis of wood structure IV: characteristics of the power spectral pattern of wood sections and application of non-microscopic wood pictures. Mem Coll Agr Kyoto Univ 138:11–23
8. Fujita M, Saito Y, Hanaoka J, Saiki H (1993) An electron diffraction method applied to the higher order structure of cellulose microfibrils (in Japanese). Bull Kyoto Univ Forest 65:325–328
9. Midorikawa Y, Fujita M (1997) Quantitative evaluation of transverse cell shapes by the Fourier transform image analysis: new expression of tracheids' shape changes in an annual ring (in Japanese). Abstracts of 47th Annual Meeting of the Japan Wood Research Society, Kochi, p 19